

TECHNICAL PAPER

JOURNAL OF THE SOUTH AFRICAN
INSTITUTION OF CIVIL ENGINEERING

Vol 57 No 3, September 2015, Pages 44–56, Paper 997



MILOŠ PERDUH graduated in 2009 from the Belgrade University with a degree in civil engineering, and he subsequently obtained a Master's degree in structural engineering. His fields of interest include finite element modelling and dynamic analyses. He has been involved in projects across Europe, the Middle East and southern Africa, and is

currently employed by AECOM SA.

Contact details:

AECOM SA (Pty) Ltd
PO Box 3173
Pretoria, 0001
South Africa
T +27 (0)12 421 3500
E: milos.perduh@aecom.com



DR BREDA STRASHEIM Pr Eng is a Senior Lecturer in Structural Engineering at Stellenbosch University. He graduated in civil engineering in 1974 and subsequently obtained a BSc in Computer Science, an M Eng, an MBA and a PhD. His professional engineering career included a period with the Department of Water Affairs, and a decade in the consulting

engineering practice of Geustyn Forsyth & Joubert Inc doing municipal infrastructure design, pipeline and dam construction and management projects, as well as business system projects. His research interests include numerical (FEA) modelling and structural dynamics. He also lectures engineering management and is involved in organising and presenting course work for the Construction Management Programme (CMP).

Contact details:

Department of Civil Engineering
Stellenbosch University
Private Bag X1
MATIELAND 7602
South Africa
T: +27 (0)21 808 4435
E: javbs@sun.ac.za

Keywords: inclined coal conveyor, Medupi, sliding joint, finite element analysis, force distribution, concrete pylon, steel gantry, simplified model

Finite element analyses of the structural behaviour of pylons supporting an inclined coal conveyor

M Perduh, J A v B Strasheim

As part of the coal conveyance system at Medupi Power Station, an inclined coal conveyor will transport coal from the stockyard to the coal transfer tower, and from there to the boilers. The conveyor is supported by concrete columns (pylons), in turn supporting the steel gantries on which the conveyor is located. The pylons can be considered as cantilever columns during the construction stage, while in the final operational stage with the steel gantries positioned in-between the pylons, a frame system will be formed. The gantries are connected to the pylons with custom-designed sliding joints, which allow limited movement of the gantries in the longitudinal direction of the conveyor. This paper describes how various finite element analyses of the structural behaviour of the pylons and the overall structure of the inclined coal conveyor were undertaken to assess wind and seismic actions. It focuses on modelling the behaviour of the concrete pylons during the construction period, a comparison between finite element models (FEMs) with different complexities and the implications of simplifying the FEMs. It will be shown that the simplified beam element models provide adequate modelling of the structural behaviour for this kind of structure. The modelling of non-linear connections between elements for static and dynamic conditions was also investigated, as well as the influence of the sliding joints between the pylons and the gantries on the overall behaviour of the structure. It will be shown that the overall behaviour of the structure can be highly influenced by the action of the sliding mechanism and that the force distribution between the structural members can differ significantly. Recommendations on how to approach the modelling of this type of structure are made.

It is concluded that the simplified model can be used to capture the behaviour of the structure, as well as the complex sliding joint mechanism, which has a major influence on the performance of the structure and the force distribution in the structural system.

INTRODUCTION

Medupi Power Station, shown in Figure 1, is situated in Lephalale, in the northern part of South Africa. After its completion it will be the fourth largest coal-fired power station in the world, and at the same time the world's largest dry-cooled coal-fired power station. The first unit should have started operation in 2014. The cost is estimated at R140 billion. It will have six generating units which, at completion, will deliver 4 788 MW of electrical power to the South African electricity distribution grid. As part of the coal conveyance system, an inclined coal conveyor (ICC) 300 metres in length, consisting of concrete pylons and steel gantries, will be installed. This paper analyses the structural behaviour of the ICC and focuses on the investigation of the required level of complexity of finite element modelling for this kind of structure during the construction and operational stages. The main focus of the investigation is pointed towards the structural behaviour and force distribution in the concrete pylons supporting the steel gantries.

SCOPE OF THE PAPER

The structure of the inclined coal conveyor was conceived as a combination of steel gantries and concrete pylons. During the construction stage, without the steel gantries in position, the concrete pylons will act as pure cantilevers in both the longitudinal and transverse directions. The paper describes the analyses of the behaviour of the concrete pylons during the construction stage. After the installation of the steel gantries, a new 'hybrid' frame system, consisting of the concrete pylons and the steel gantries, will be formed in the direction of the conveyor. The paper also describes the finite element (FE) analyses that were done of the behaviour of the complete ICC structure. A number of FE models with different levels of complexity were created and their advantages and disadvantages are given. The connections between the steel gantries and the concrete pylons are designed to allow a certain amount of longitudinal movement of the steel gantries, thus avoiding the development of any additional



Figure 1 Medupi Power Station (Source: Eskom)

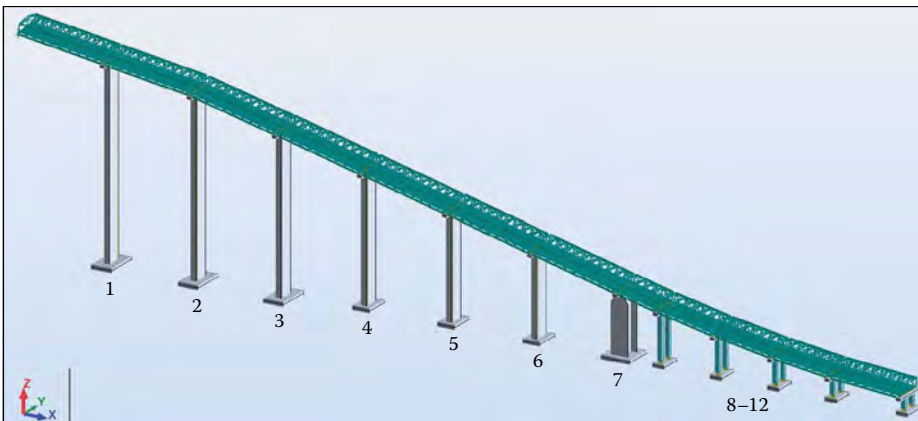


Figure 2 Three-dimensional view of FE model of inclined coal conveyor

forces in the system due to the effects of changes in temperature. With the aid of finite element software, the designer and analyst went through a process to discover and evaluate differences in behaviour of the structural system with and without implementation of the sliding connection between the pylons and the gantries.

The paper focuses on the following aspects of the structural analysis:

- **Investigation into the behaviour of the concrete pylons during the construction period:** Being tall and slender structures, the concrete pylons are vulnerable to possible cross-wind vortex-shedding effects. The amplitude of the additional bending moments induced by the vortex-shedding effects was quantified. The temporary measures undertaken to secure the structural stability of the concrete pylons during the construction period were also analysed.
- **Comparison of results from FE models with different complexities:** A number of different FE models were created using different types of elements, e.g. beams

and shells. It was necessary to determine whether the steel gantries, which are actually 3D trusses, could be modelled with a single beam element, and to what aspects of the modelling special attention needed to be paid. The results from the different FE models and the different analyses, both static and dynamic, are presented and compared. The aim was to investigate whether simplified FE models, with only beam elements modelling the behaviour of the 3D trusses, could fully describe the behaviour of this type of structure. The advantages and disadvantages of using FE models with different levels of complexity are discussed.

- **Modelling of the non-linear sliding connection between steel gantries and concrete pylons:** Using the implemented non-linear gap elements of the FE software, the behaviour of the structure was simulated under static loading. Based on the results of this analysis, the replacement of the non-linear gap elements with linear elements was attempted. A model of a sliding connection with a finite gap

which can be used for modal analyses was required in view of the fact that non-linear gap elements cannot be used in modal analysis.

- **Investigation into the influence of the sliding connection on the overall behaviour of the structure:** A number of FE models of the concrete pylons for the systems with and without sliding connections were analysed and the results are compared. Special attention was paid towards both the structural behaviour of the tallest pylons and the stiff, braced (seventh) pylon. It is shown that the sliding connections have a major influence on the behaviour of the pylons.
- **Modelling the effects of cracking of the pylon box section:** In addition, the analyses of the concrete pylons with both cracked and uncracked sections were compared. It is important to determine the influence of the implementation of properties of cracked sections in FE models on the overall behaviour of the structure. Both the periods of oscillation and the force distribution will differ due to cracking of the sections.

STRUCTURAL SYSTEM AND COMPONENTS

Structural concept of the inclined coal conveyor

The ICC will transport coal from the stockyard to the coal transfer tower, and from there to the boilers. Two conveyors in the power station will supply coal for six generating units. The structural system of the ICC consists of steel bridge gantries spanning 12 concrete pylons (Figure 2). The spans of the steel bridge gantries vary from 14 m to 30 m. The height of the pylons varies from 3 m to 60 m. The cross-section of the first six pylons is a hollow box section with outside dimensions of 5 800 mm × 2 000 mm, while the seventh pylon is stiffened with additional walls and has total outside dimensions of 5 800 mm × 5 800 mm (Figure 3). The thickness of the walls is constant throughout at 400 mm. The pylons are founded on individual pad footings, with a depth of 1 500 mm. The steel bridge gantries supporting the coal conveyors consist of rigid steel portal frames, supported on two main steel trusses. The width of the steel gantries is 9.5 m, while the height is 4.5 m (an isometric view of one typical steel gantry is shown in Figure 4).

The pylons indicated are numbered from left to right from 1 to 12. This paper focuses mainly on analyses of the behaviour of the

first three pylons, which are the tallest, and the seventh one, which is the stiffest. For reference, the global X-direction is along the length of the conveyor and the global Y-direction is perpendicular to the direction of the conveyor, as shown in Figure 2.

Design philosophy of structural system

The static structural system formed by the pylons during the construction stage is equivalent to a pure vertical cantilever in all directions. Once the steel bridge gantries have been positioned between the pylons, a new frame is formed in the longitudinal direction. In this case the steel bridge gantries not only have the function of spanning between the pylons to support the coal conveyors, but also act as a continuous strut-tie link between the pylons, forming a key element for stability of the pylons in the longitudinal X-direction. In the transverse Y-direction the pylons will always perform as cantilevers, due to the small flexural stiffness of the gantries in that plane. The sliding connections between the pylons and the top end of each steel gantry allow limited free movement of the gantries. This means that, during operational conditions, the concrete pylons will be subjected to only vertical reactions from the steel gantries. However, during strong winds and seismic activity, when the movement of the pylons in the longitudinal direction of the conveyor is larger than the gap provided in the sliding connection at the gantry supports, the sliding mechanism will lock, and the steel gantries with the pylons will perform as a frame system.

The gantry support sliding and locking mechanism

Figure 5 shows the connection with the sliding mechanism between the pylons and steel gantries. The lower parts of each steel gantry, outlined in blue, are restrained from free movement and are fully pinned in all three global directions. The top parts of each steel gantry, outlined in red, have a sliding connection, but only in the global X-direction. The contact surfaces of the sliding connections, which have slotted holes, are made of Teflon. Taking into account that the static and kinetic friction coefficients between Teflon surfaces are both 0.04, the friction forces can be neglected. This means that the top part of the steel gantry has a sliding support with a finite sliding length. If the size of the movement reaches the size of the allowable gap, the sliding mechanism will lock and neighbouring pylons will be linked. Therefore the steel gantry between these pylons will then

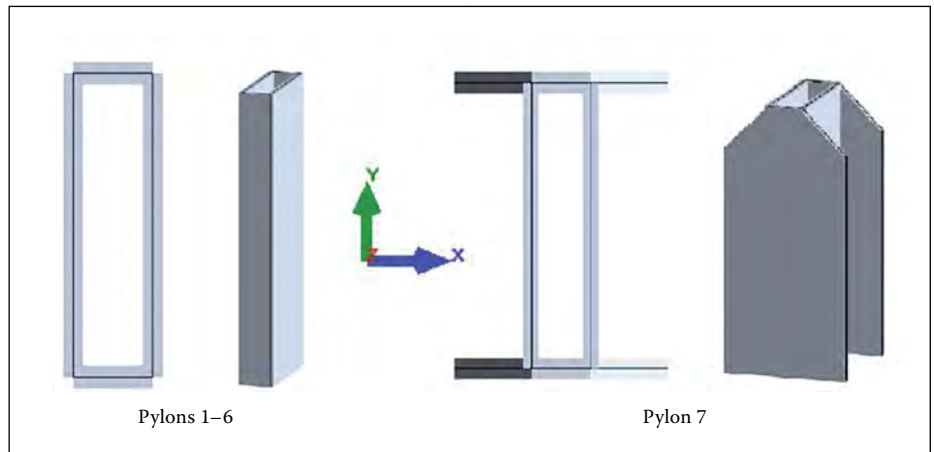


Figure 3 Plan layout and 3D view of typical pylon sections



Figure 4 Isometric view of typical steel gantry

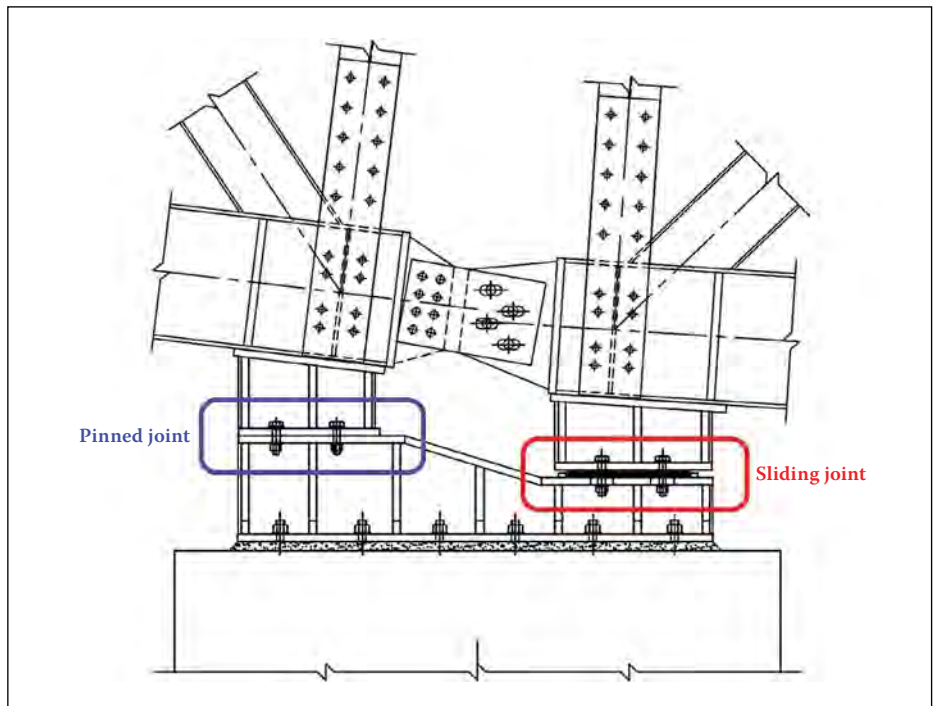


Figure 5 Sliding mechanism at gantry supports

play the role of a strut or a tie, depending on the loading condition.

Due to the specific environment in which the structure will operate, and keeping in mind the strategic importance of the structure, the design engineers decided to consider two extreme conditions for the

structural analysis – the first one where the friction coefficient is equal to zero, and the second one where the friction coefficient is equal to one. This is justified considering that the operational life and the maintenance of the sliding connection cannot be explicitly estimated.

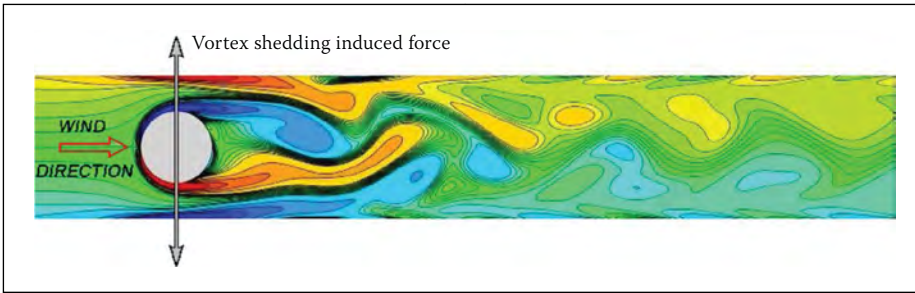


Figure 6 Vortex-shedding phenomenon

Table 1 Vortex-shedding results for the three tallest pylons

| Pylon | Direction | Mode | Frequency (Hz) | b (m) | St number | V_b (m/s) | V_{crit} (m/s) | V_{crit}/V_b |
|---------|-----------|--------|----------------|-------|-----------|-------------|------------------|----------------|
| Pylon 1 | X | Mode 1 | 0.33 | 5.8 | 0.06 | 20 | 31.90 | 1.60 |
| | Y | Mode 1 | 0.76 | 2 | 0.12 | 20 | 12.67 | 0.63 |
| Pylon 2 | X | Mode 1 | 0.38 | 5.8 | 0.06 | 20 | 36.73 | 1.84 |
| | Y | Mode 1 | 0.88 | 2 | 0.12 | 20 | 14.67 | 0.73 |
| Pylon 3 | X | Mode 1 | 0.48 | 5.8 | 0.06 | 20 | 46.40 | 2.32 |
| | Y | Mode 1 | 1.1 | 2 | 0.12 | 20 | 18.33 | 0.92 |

LOAD ANALYSIS

Operational load cases

For the design of the structure during the normal operational stage, the following main load cases were considered:

- Self-weight load – main and secondary structural elements, conveyors, material and water pipes
- Imposed load – service and operating personnel loads, live load from conveyors and belt tensioning forces
- Wind load
- Seismic load
- Loading due to temperature gradient.

Load cases analysed for the construction stage

During the construction stage the pylons will be freestanding and possibly be vulnerable to strong winds. The SANS loading code (SANS 0160-1989) does not deal with loadings from the effects of gusts of wind and therefore two additional internationally recognised and accepted codes were consulted. These were the CICIND 2001 *Model code for concrete chimneys* (CICIND 2001) and Eurocode 1991-1-4 (EN 1991). The following two wind loading effects were considered:

Along-wind loading

The along-wind loading of a structure due to buffeting by wind can be assumed to consist of a basic component based on the mean hourly wind speed and a fluctuating component due to wind speed variations from the mean. The dynamic response of a structure in the along-wind direction can be predicted with reasonable accuracy by the

gust factor approach, provided the wind flow is not significantly affected by the presence of neighbouring tall structures or the surrounding terrain. The method described in the CICIND *Model code for concrete chimneys* (CICIND 2001) was used to calculate the along-wind effects.

The mean hourly wind load at height z is:

$$w_m(z) = 0.5\rho_a v(z)^2 C_D d(z) \quad (1)$$

where ρ_a is the density of air, $v(z)$ is the wind speed at height z , C_D is a shape factor and $d(z)$ is the width of the pylon.

The wind load due to gusts was determined by:

$$w_g(z) = \frac{3(G-1)z}{h^2} \int_0^h w_m(z) z dz \quad (2)$$

where G is the gust factor, h is the height of the top of the structure above ground level and z is the height above ground level.

Across-wind loading: Vortex-shedding dynamic action

Vortex-shedding occurs when wind airflow vortices are shed alternately from opposite sides of the pylons, as shown in Figure 6. This is an additional loading of the structure acting in the transverse direction. This effect can occur at relatively low wind speeds and gives rise to a fluctuating load perpendicular to the wind direction. Structural vibrations may occur if the frequency of vortex-shedding is close to any of the natural frequencies of the pylons.

The vortex-induced loading calculations were done according to the Eurocode

1991-1-4 (EN 1991). The effects of vortex-shedding do not need to be investigated if the critical wind velocity $V_{crit,i}$ is larger than 1.25^*V_m , where V_m is the 10-min mean wind velocity at the cross-section where vortex-shedding occurs.

The formula for the critical wind velocity for vortex-shedding is:

$$V_{crit,i} = \frac{bn_{i,y}}{St} \quad (3)$$

where b is the reference width of the cross-section at which resonant vortex-shedding occurs, $n_{i,y}$ is the natural frequency of the considered flexural mode i of the cross-wind vibration and St is the Strouhal number.

To calculate the first natural frequency of a uniformly loaded cantilever beam with a concentrated mass attached to the free end, the following formula based on the Rayleigh method can be used:

$$n1 = \frac{1}{2\pi} \sqrt{\frac{k}{M + 0.23m}} \quad (4)$$

where $k = \frac{3EI}{l^3}$, l is the beam length,

E is Young's modulus of elasticity, I is the moment of inertia, m is the mass of the whole beam and M is the mass attached to the free end.

The results for the first three pylons are shown in Table 1. The locations where vortex-shedding is identified as a potential problem are shown in red, implying that the three tallest concrete pylons may experience forces induced by vortex-shedding effects during the construction stage.

The pylons are designed for the operational condition when all elements, including the gantries, are in place. It was determined that it will not be economical to design all the elements for the temporary load conditions, but rather to provide additional temporary supports during the construction stage. It was thus decided to use normal post-tensioned cables to support the pylons during construction, as shown in Figure 7.

Four cables were provided on each side of the first three pylons. Each cable was post-tensioned to 100 kN. It is estimated that the maximum load in the cables during dynamic wind effects will increase to 150 kN per cable. The cables are anchored to adjacent foundations and temporary stress blocks. Introduction of the cables changed the static system of the pylons from a pure cantilever to that of a continuous beam with elastic support. Therefore, the natural frequencies of the pylons changed and had to be recalculated. One elegant way to calculate the natural

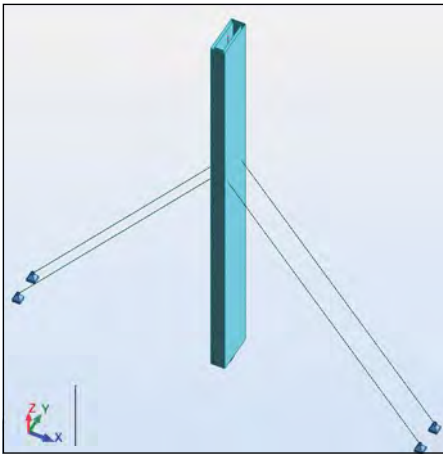


Figure 7 Stayed pylon

frequency is to use FE software. The problem was that the available FE software at that time did not support modal analysis with geometric non-linear cable elements. The easiest way to address this problem was to replace the cable element with an elastic support that had the same stiffness as the cable element. Table 2 contains a summary of forces in the pylons due to the wind load during the construction stage. It can be seen that the bending moments about the global Y-direction, caused by the wind acting in the global X-direction, are reduced by 30% with the implementation of the cables. The calculated axial force in the cable elements was smaller than the expected maximum of 150 kN.

Seismic actions during construction

After locating the site on the seismic hazard map from SANS 0160-1989 (SANS 1989), it was decided to use a ground peak acceleration of 0.05 g. The normalised response spectrum is shown in Figure 8. The client requested that the behaviour of the structure should remain elastic during seismic activity and therefore the seismic behaviour factor used in this case is equal to one. The pylons

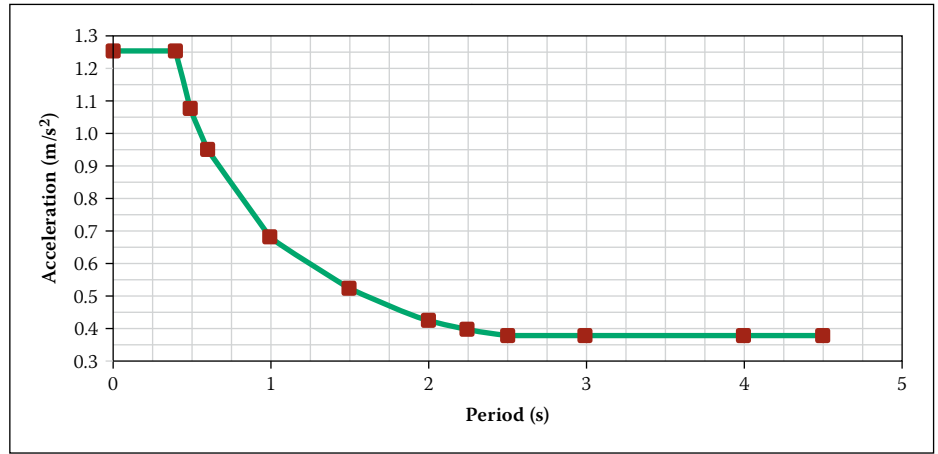


Figure 8 Normalised response spectrum (a = 0.05 g)

Table 2 Summary of forces in the pylons from wind loads during construction

| Loading/Pylon | Pylon 1 | Pylon 2 | Pylon 3 |
|--|---------|---------|---------|
| Total axial load (SLS) on base (kN) | 8 781 | 8 192 | 7 261 |
| Along-wind moment My (SLS) on base (kNm) | 16 010 | 13 878 | 10 085 |
| Vortex moment Mx (SLS) on base (kNm) | 10 147 | 9 021 | 7 428 |
| ULS axial load (unstayed) (kN) | 8 781 | 8 192 | 7 261 |
| ULS bending moment My (unstayed) (kNm) | 26 730 | 22 986 | 16 531 |
| ULS bending moment Mx (unstayed) (kNm) | 16 235 | 14 434 | 11 885 |
| Capacity factor | < 1 | < 1 | 1.14 |
| ULS axial load (stayed) (kN) | 9 410 | 8 815 | 7 883 |
| ULS bending moment My (stayed) (kNm) | 17 917 | 15 853 | 11 618 |
| ULS bending moment Mx (stayed) (kNm) | 16 235 | 14 434 | 11 885 |
| Capacity factor | 1 | > 1 | > 1 |

SLS – Serviceability Limit State; ULS – Ultimate Limit State
 F(x, y or z) – force in X, Y or Z direction; M(x or y) – moment about X, Y or Z axis

are also vulnerable to possible seismic action during the construction stage, especially in the longitudinal direction of the conveyor before the steel gantries are in their final position.

Table 3 shows the results from the seismic analyses for the first three and for the seventh pylon. The complete quadratic combination (CQC) method of modal combination was used. It is important to have

Table 3 Seismic analysis results for Pylons 1, 2, 3 and 7

| Model | | Beams | | | | | Shells | | | | |
|-------------------|-------------------|---------|---------|---------|----------|----------|---------|---------|---------|----------|----------|
| Direction | | X | | | Y | | X | | | Y | |
| Column/Cases/Info | | Fx (kN) | Fy (kN) | Fz (kN) | My (kNm) | Mx (kNm) | Fx (kN) | Fy (kN) | Fz (kN) | My (kNm) | Mx (kNm) |
| Pylon 1 | 1.0°DLL+1.0°S(X+) | 319 | 0 | 9 204 | 10 988 | 0 | 315 | 0 | 9 039 | 10 787 | 0 |
| | 1.0°DLL+1.0°S(Y+) | 0 | 445 | 9 204 | 0 | 17 159 | 0 | 435 | 9 039 | 0 | 17 135 |
| Pylon 2 | 1.0°DLL+1.0°S(X+) | 308 | 0 | 8 585 | 9 611 | 0 | 306 | 0 | 8 419 | 9 405 | 0 |
| | 1.0°DLL+1.0°S(Y+) | 0 | 434 | 8 585 | 0 | 16 239 | 0 | 428 | 8 419 | 0 | 16 325 |
| Pylon 3 | 1.0°DLL+1.0°S(X+) | 292 | 0 | 7 611 | 8 291 | 0 | 282 | 0 | 7 776 | 8 359 | 0 |
| | 1.0°DLL+1.0°S(Y+) | 0 | 438 | 7 611 | 0 | 14 921 | 0 | 422 | 7 776 | 0 | 14 739 |
| Pylon 7 | 1.0°DLL+1.0°S(X+) | 445 | 0 | 4 677 | 6 392 | 0 | 462 | 0 | 4 919 | 6 899 | 0 |
| | 1.0°DLL+1.0°S(Y+) | 0 | 474 | 4 677 | 0 | 6 596 | 0 | 496 | 4 902 | 0 | 7 107 |

DLL – dead load; S(X± or Y±) – seismic load in ± X or ± Y direction; F(x, y or z) – force in X, Y or Z direction; M(x, y or z) – moment about X, Y or Z axis

Table 4 Pylon 1 forces and seismic capacity

| Loading/Pylon | Pylon 1 (1.6°SX+0.48°SY) | Pylon 1 (0.48°SX+1.6°SY) |
|---------------------------------------|--------------------------|--------------------------|
| Total axial load (SLS) on base (kN) | 8 781 | 8 781 |
| Seismic moment My (SLS) on base (kNm) | 10 988 | 10 988 |
| Seismic moment Mx (SLS) on base (kNm) | 17 159 | 17 159 |
| ULS axial load (kN) | 8 781 | 8 781 |
| ULS bending moment My (kNm) | 17 596 | 5 274 |
| ULS bending moment Mx (kNm) | 8 236 | 27 454 |
| Capacity factor | > 1 | > 1 |

S(X or Y) – seismic load in X or Y direction; M(x or y) – moment about X or Y axis

Table 5 Periods of oscillation

| Model | Beams | |
|---------|-------|-------|
| | X | Y |
| Pylon | T (s) | T (s) |
| Pylon 1 | 3.05 | 1.3 |
| Pylon 2 | 2.66 | 1.14 |
| Pylon 3 | 2.1 | 0.91 |
| Pylon 7 | 0.23 | 0.19 |

over 90% of the modal mass participating to model the dynamic response realistically. The results from two different models, the model in which the pylons are modelled with beam elements, and the model in which the pylons are modelled with shell elements, are compared. The results of the two models differ by from less than 1% up to 8%. Table 4 shows the ultimate forces for the design of Pylon 1.

In order to check the FE analysis results, additional hand calculations were performed. The same formula based on the Rayleigh method (Equation 4) was used to calculate

the period of oscillation of the cantilever beam with a point mass at the free end. The results are identical. The modal analysis for seismic loadings was done without modelling of the cable elements. The reason behind this was that the analyst could not be sure that the temporary stress blocks, used to anchor the cables, would remain in position during seismic activity. Therefore, the influence of the cables was ignored.

From Table 3 it can be seen that for the first three (tallest) pylons, the moments about the global X-axis are much higher than those around the global Y-axis. This is to be expected, because the moment of inertia around the global X-axis is much higher. Therefore, the section is stiffer in that plane and the period of oscillation is shorter, as is shown in Table 5. As a result of the shorter period of oscillation, the pseudo-acceleration is higher and the lateral force induced by inertia is larger, causing higher moments at the base. For the seventh pylon, the periods of oscillation are almost identical, which is reflected by the very close values of the bending moments at the base.

From a comparison of the bending moments, due to the wind and seismic load analyses, it can be seen that the forces due to the wind loading are much higher than those due to the seismic loading. This means that, during the construction stage, for this type of structure and ground peak acceleration of 0.05 g, the wind loading is most probably the critical loading.

FINITE ELEMENT MODELLING

Modelling of the pylons and the gantries

In order to investigate the behaviour of the structure during seismic activity, finite element models (FEM) with different levels of complexity were created using the Autodesk Robot Structural Analysis Professional package (Autodesk). The sliding mechanism at the gantry support gaps was not incorporated in the following FEMs:

- Model A: FEM with only beam elements. The pylons and the steel gantries are modelled with single beam elements. This model allows a quick overview of all types of results (Figure 9).
- Model B: FEM in which the pylons are modelled with shell elements and the steel gantries are modelled with single beam elements. This model provides localised results for the pylons. Shear lag effects in the pylons can be quantified.
- Model C: FEM in which the pylons are modelled with single beam elements and the steel gantries are modelled as 3D space trusses, with full complexity. This model shows the effects of the 3D truss system. Because the steel gantries cannot displace or expand in the longitudinal

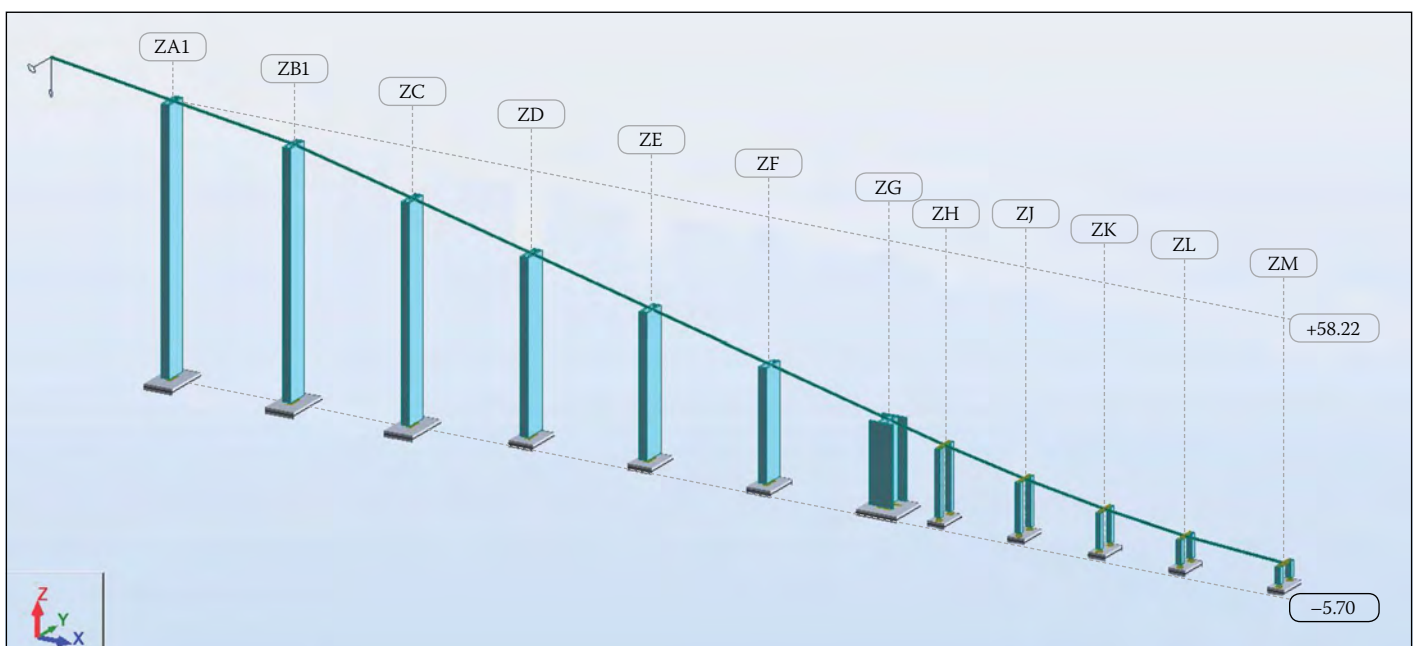


Figure 9 FE model with single-beam elements

direction for this FEM, horizontal forces from the gantries are transferred to the pylons.

- Model D: FEM with full 3D modelling. The pylons are modelled with shell elements and the steel gantries are modelled as space trusses. This is the most complex FE model (Figure 10).
- Model E: FEM with only one pylon, the tallest one. The rest of the structure is represented by a single spring support which has stiffness identical to the replaced parts of the structure. The results from this very simplified model differed by less than 10% from the results from the more complex models. This type



Figure 10 Detail from FE model with shells and 3D gantries

Table 6 Modal results from four different FE models

| Model | Model A (beams) | | | | Model B (shells + beams) | | | | Model D (full 3D model) | | | | Model C (3D truss + beams) Gantries + Beams | | | |
|----------------|-----------------|----------|----------|----------|--------------------------|----------|----------|----------|-------------------------|----------|----------|----------|--|----------|----------|----------|
| | X | | Y | | X | | Y | | X | | Y | | X | | Y | |
| Modes/ Info | T (s) | M (%) | T (s) | M (%) | T (s) | M (%) | T (s) | M (%) | T (s) | M (%) | T (s) | M (%) | T (s) | M (%) | T (s) | M (%) |
| Mode 1 | 1.52 | 52.91 | 1.27 | 36.42 | 1.58 | 53.93 | 1.34 | 37.14 | 1.56 | 54.63 | 1.4 | 35.38 | 1.51 | 54.83 | 1.33 | 34.23 |
| Mode 2 | 0.65 | 54.13 | 0.84 | 42.55 | 0.69 | 54.73 | 0.87 | 43.08 | 0.69 | 55.09 | 0.98 | 40.7 | 0.65 | 55.66 | 0.94 | 39.84 |
| Mode 3 | 0.56 | 56.42 | 0.6 | 50.51 | 0.6 | 56.2 | 0.62 | 51.38 | 0.6 | 55.91 | 0.76 | 49.29 | 0.56 | 57.18 | 0.73 | 48.68 |
| Mode 4 | 0.48 | 69.54 | 0.45 | 52.56 | 0.51 | 69.16 | 0.46 | 51.44 | 0.51 | 69.75 | 0.62 | 50.72 | 0.48 | 69.91 | 0.6 | 50.73 |

T – period of oscillation; M – mass participation

Table 7 Seismic results from four different FE models

| Model | | Model A (beams) | | | | | Model B (shells + beams) | | | | |
|------------------|-------------------|-------------------------|------------|------------|-------------|-------------|----------------------------|------------|------------|-------------|-------------|
| Pylon/Cases/Info | | Fx (kN) | Fy (kN) | Fz (kN) | Mx (kNm) | My (kNm) | Fx (kN) | Fy (kN) | Fz (kN) | M (kNm) | My (kNm) |
| Pylon 1 | 1.0*DLL+1.0*S(X+) | 320 | 0 | 11 185 | 0 | 6 308 | 305 | 0 | 11 339 | -22 | 6 240 |
| | 1.0*DLL+1.0*S(X-) | -321 | 0 | 11 065 | 0 | -6 371 | -305 | 0 | 11 218 | -24 | -6 242 |
| | S(X+) | 321 | 0 | 60 | 0 | 6 340 | 305 | 0 | 60 | 1 | 6 241 |
| | S(X-) | -321 | 0 | -60 | 0 | -6 340 | -305 | 0 | -60 | -1 | -6 241 |
| | 1.0*DLL+1.0*S(Y+) | -1 | 444 | 11 125 | 15 088 | 32 | 0 | 430 | 11 278 | 14 807 | 33 |
| | 1.0*DLL+1.0*S(Y-) | -1 | -444 | 11 125 | -15 088 | 32 | 0 | -430 | 11 278 | -14 807 | 33 |
| | S(Y+) | 0 | 444 | 0 | 15 088 | 0 | 0 | 430 | 0 | 14 807 | 0 |
| | S(Y-) | 0 | -444 | 0 | -15 088 | 0 | 0 | -430 | 0 | -14 807 | 0 |
| Model | | Model D (full 3D model) | | | | | Model C (3D truss + beams) | | | | |
| Pylon/Cases/Info | | Fx (kN) | Fy (kN) | Fz (kN) | Mx (kNm) | My (kNm) | Fx (kN) | Fy (kN) | Fz (kN) | Mx (kNm) | My (kNm) |
| Pylon 1 | 1.0*VL+1.0*S(X+) | 354 | 30 | 11 441 | -612 | 9 381 | 365 | 0 | 11 000 | 0 | 9 627 |
| | 1.0*VL+1.0*S(X-) | -253 | 29 | 11 321 | -619 | -2 842 | -257 | 0 | 11 115 | 0 | -2 793 |
| | S(X+) | 303 | 0 | 60 | 3 | 6 112 | 311 | 0 | 58 | 0 | 6 210 |
| | S(X-) | -303 | 0 | -60 | -3 | -6 112 | -311 | 0 | -58 | 0 | -6 210 |
| | 1.0*VL+1.0*S(Y+) | 33 | 313 | 11 163 | 16 448 | 3 195 | 54 | 418 | 11 057 | 17 169 | 3 417 |
| | 1.0*VL+1.0*S(Y-) | 32 | -351 | 11 157 | -16 416 | 3 193 | 54 | -418 | 11 057 | -17 169 | 3 417 |
| | S(Y+) | 0 | 332 | 3 | 16 432 | 1 | 0 | 418 | 0 | 17 169 | 0 |
| | S(Y-) | 0 | -332 | -3 | -16 432 | -1 | 0 | -418 | 0 | -17 169 | 0 |

VL – vertical load; S(X± or Y±) – seismic load in ± X- or ±Y direction; F(x, y or z) – force in X, Y or Z direction; M(x or y) – moment about X or Y axis

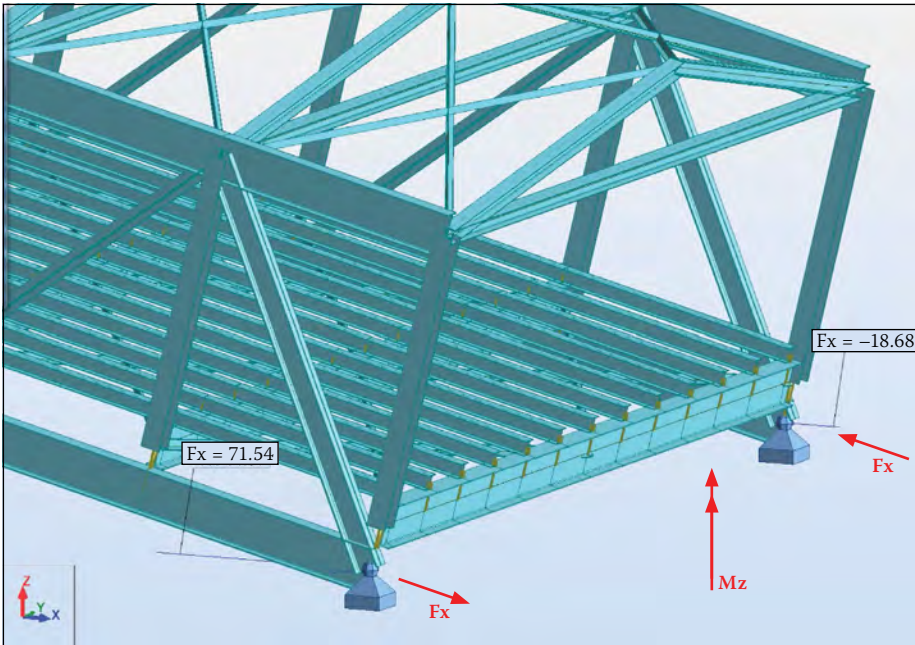


Figure 11 3D truss effects

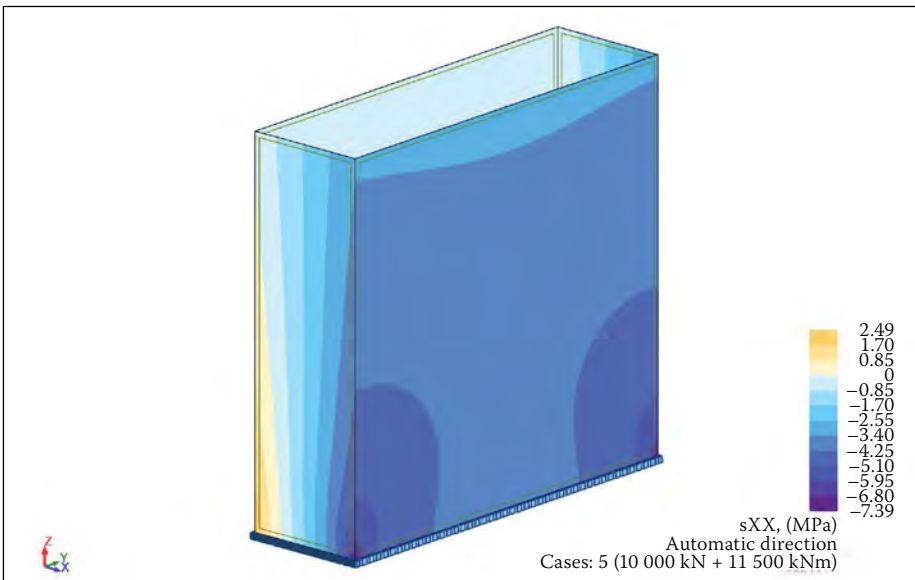


Figure 12 Shear lag effects

of FE model can be used for preliminary design and sizing of the concrete pylons. It can, however, not be used for structures with sliding connections.

Selection of FE models based on comparison of results from the different FE models

The modal analysis results, the vibration period (in seconds) and the mass participation factors (in %) for the first four modes, from the above-mentioned FE models with elastic supports, are shown in Table 6. The X-direction is in line with the longitudinal direction of the conveyor, while the Y-direction is perpendicular to it. The results from the modal analyses from four different models are very close, supporting the use of simplified models for this type of analysis.

Table 7 contains the results for the first pylon from the seismic analyses. These show

different magnitudes of the moments about the Y-axis (M_y) for the load combinations of the models with gantries represented by one single beam element (Models A and B), and the models with full 3D gantries (Models C and D). It can be seen that the results for the seismic actions in the longitudinal direction (X) are almost identical. The results for load combinations (VL + SX) differ between the models in which the gantries are represented by a single beam element (Models A and B), and those in which the gantries are modelled as 3D trusses (Models C and D). The differences in the tabulated results are caused by the load distribution effects of the 3D trusses. The gantries transfer the horizontal reaction to the pylons. These effects should not be omitted for modelling purposes. By studying the results for the seismic response in the Y-direction it can be seen that they vary by up to 10%. This exercise supported

the thesis that for further analyses only two FE models, i.e. the model with single beam elements (Model A) and the model with single beam elements and 3D gantries (Model C) need to be used.

Modelling of soil-structure interaction

To simulate realistic soil-structure interaction, the bases with elastic planar supports were modelled. One of the advantages of models with planar supports is that the designer and the analyst can quickly determine whether some parts of the bases are subject to uplifting and, if that is the case, they can perform a non-linear analysis. By performing a non-linear analysis with contact elements between the bases and the soil, it is possible to model the no-tension condition between the soil and the bases.

In all FE models presented the elastic stiffness coefficient for the discretisation model of the soil $k_v = 200\,000\text{ kN/m}^3$ was used.

Implications of simplified FE models

For the FEM with single beam elements it is crucial to calculate the correct axial and flexural stiffness of the beams that represent the steel gantries. If the stiffness of the beams is not correct, the overall behaviour of the whole structure and the force distribution between the pylons will not be the same as in the full 3D FE model. To model the effect of the space truss system correctly, rotation of the beams in the model around the global Z-axis must not be allowed. As shown in Figure 11, the steel gantry acts as a fixed beam and can attract moment around the global Z-direction. This moment (M_z) can be replaced by force couple (F_x), as shown in Figure 11.

The advantages and disadvantages of using a simplified FE model with only beam elements are:

- Computing time is faster, inputting is easier, changes can be made to the model and the results can be checked more rapidly. Most FE packages allow easy and individual review of all beam element axial, bending, shear and torsion section forces.
- For shell elements only total resultant stress can be reviewed. It is not easy to determine what portion of the total stress can be attributed to bending or axial stresses. Modern versions of FE packages provide a solution by which different shell elements can be grouped together as a single element. The software is then able to compute and present the overall force results for the whole element – in this particular case the whole rectangular hollow section of the pylons.

■ An FE model with beam elements can be used to compute global section results. Then analysis with another FE model with shell elements and a fine mesh can be performed, and the results from the previous model can serve as an input. This micro-modelling allows checking of possible shear lag effects in stiff portions of the rectangular hollow section of the pylons (Figure 12).

Modelling of the sliding connection at the gantry supports using gap elements

Analyses with gap elements were done to model the realistic behaviour of the structure which has special locking devices at the gantry supports. This means that the first pylon will deform before the allowable gap is reached and it will then link with the second pylon. This new system must then deform until it links with the third pylon and so on. In the Autodesk Robot Professional (Autodesk) structural analysis program there is an option to model gap elements directly and this can be used for static analyses (Figure 13). However, these elements cannot be used to perform dynamic modal analyses because the natural frequency solver allows only one stiffness value to be used at the connection. The modelling of the non-linear behaviour where the beam has the freedom to move along the slot (very low stiffness) and then reach the gap end (very high stiffness) is not possible in a modal analysis. To overcome this problem, short 'soft' beam elements, with the same length as the gap, were used to model the physical gap elements. In order to model the correct stiffness of these beams, an iterative process was performed. The method used was to create a model with automatic gap elements and then to create another separate model with soft beams. A number of iterations with different axial stiffnesses of the soft beams were performed until the deformation and forces in the two models were identical.

For FEM software packages that do not support the concept of gap elements the following analysis can be performed to model the behaviour of a frame with three pylons.

- Step 1: Decide what is the allowable sliding length (say a).
- Step 2: Model only one pylon and apply force P at the top of it, which will cause deflection of the pylon equal to a . Record the forces in the pylon.
- Step 3: Model two pylons linked by a beam with the same stiffness as the steel gantry and apply force Q at the top of the first pylon, which will cause deflection of the second pylon equal to a . Record the forces in the pylons.
- Step 4: Model three pylons with beams between them and apply force R at the

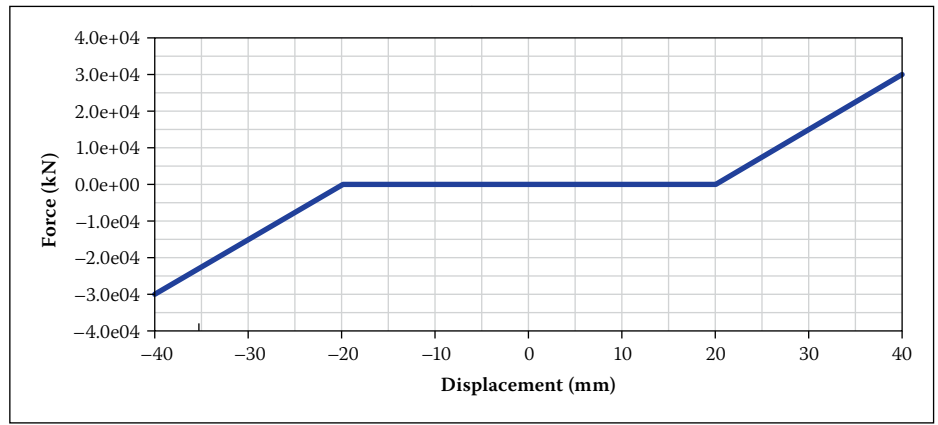


Figure 13 Non-linear model of gap element

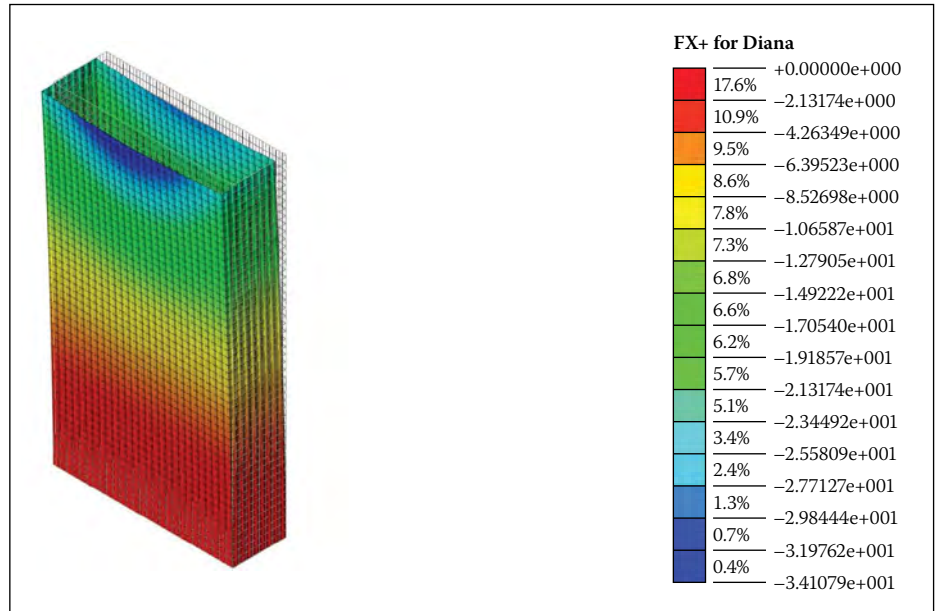


Figure 14: FEM of the pylon from TNO-Diana

Table 8 Control calculations for the gap elements

| Step | Column 1 | | Column 2 | | Column 3 | |
|--------|----------|---------|----------|---------|----------|---------|
| | u (mm) | M (kNm) | u (mm) | M (kNm) | u (mm) | M (kNm) |
| Step 2 | 20 | 21 305 | n/a | n/a | n/a | n/a |
| Step 3 | 21.3 | 22 703 | 20 | 21 330 | n/a | n/a |
| Step 4 | 6 | 6 368 | 25.3 | 5 662 | 5 | 5 320 |
| Sum | 47.3 | 50 376 | 45.3 | 26 992 | 5 | 5 320 |

- top of the first pylon. Run the analysis and record the deflections and forces in the pylons. The total deflections and forces of the pylons will be equal to the sum of the results from all three models.
- Step 5: Create a model with three pylons and the beams between them. Divide each beam into two beams and make one of them the same length as a . Apply a force equal to the sum of the forces P , Q and R , and adjust the stiffness of the short beams (length equal to a) until the results are identical with those from the model with gap elements.

A similar process has to be applied for larger frames. To test this approach a number of

frames with three columns were created. Table 8 shows the results for the analytical hand calculation of the frame with gaps. Table 9 shows the results for the three different frames. The first row presents results for the frame with automatic gap elements, the second one is for the frame with soft beams (hand gap) and the third one is for the frame with no gap elements. The results for the frames with gap elements are almost identical with those for the analytical hand calculations. The difference between the moments in the columns for frames with and without gap elements is obvious. The moment in the first column increases, while the moment in the last column decreases when using gap elements.

Table 9 Results from the testing of the gap elements

| Model | Column 1 | | Column 2 | | Column 3 | |
|----------|----------|---------|----------|---------|----------|---------|
| | u (mm) | M (kNm) | u (mm) | M (kNm) | u (mm) | M (kNm) |
| Auto gap | 47.3 | 50 388 | 25.3 | 26 984 | 5 | 5 316 |
| Hand gap | 47.3 | 50 436 | 25.3 | 26 965 | 5 | 5 287 |
| No gap | 28.5 | 30 351 | 25.3 | 26 984 | 23.8 | 25 353 |

Table 10 Summary of results for analyses of section cracking

| Case | Forces/Model | | Linear | Non-linear | u, lin/u, nlin |
|--------|--------------|--------------|-------------|--------------|----------------|
| | Axial (kN) | Moment (kNm) | u, lin (mm) | u, nlin (mm) | (%) |
| Case 1 | 10 000 | 5 000 | 3.15 | 13.12 | 24 |
| Case 2 | 10 000 | 8 000 | 5.03 | 21.79 | 23 |
| Case 3 | 10 000 | 10 000 | 6.3 | 28.74 | 22 |
| Case 4 | 10 700 | 11 500 | 7.23 | 34.11 | 21 |

In the analysis of the ICC behaviour with FE models, replacement of the automatic gap elements with soft beams was done using the following steps:

- Step 1: Create a version of Model A, A1, an FE model with beam elements, implement automatic gap elements and apply seismic load as equivalent static load (assume some period of oscillation).
- Step 2: Create a version of Model A, A2, an FE model with beam elements and soft beams. Apply seismic load as in Step 1. Adjust the stiffness of the soft beams to have more or less the same deformations and forces in the elements as in the model with automatic gap elements.
- Step 3: Run modal and seismic analyses with the FE model with soft beams. Compare the assumed periods of oscillation with the computed ones. If they are different, repeat the process from Step 1 onwards with new periods of oscillation (using different periods of oscillation for each pylon, because by studying the results from the modal analyses it can be

seen that the different groups of pylons oscillate with different periods).

In order to compare the results from Robot, an identical FE model of the structure with soft beams was created in the Strand7 FEM package (Strand7 Software). The results from the modal analyses were identical.

Modelling of the behaviour of the cracked concrete pylon box section

To calculate the effective stiffness of a cracked hollow box pylon section, micro material modelling was performed with the Diana FE software (TNO Diana). Two models were created, one with linear and one with non-linear materials (Figure 14). Both materials, i.e. the concrete and the steel reinforcement, were modelled using the material non-linear formulation. To estimate the net effective stiffness of the cracked sections, deflections from these two models were compared, and the results are presented in Table 10.

As shown in Table 10, four different load cases were analysed. An almost identical axial force is combined with different bending

moments to model and predict the behaviour of a cracked reinforced concrete section. As expected, the deflections of the cracked sections are between four and five times bigger than those of the uncracked sections. To predict the behaviour of the structure with cracked sections, and using for the pylons an estimated effective stiffness of 22.5% of the total elastic stiffness, another seismic analysis was done, and these results are shown in Table 11. As expected, the oscillation periods were longer.

By comparing the values of the moments for the first two pylons, it can be seen that the moments from the analysis with reduced stiffness are about 30% smaller. This is because the oscillation period is longer and therefore the applied lateral seismic force is smaller. The pylons with reduced stiffness will deform more and therefore close the sliding gap 'faster' than the pylons with full stiffness.

If behaviour factors are introduced to estimate the inelastic deformation in the concrete pylons, the same behaviour factor should not be used for all pylons because:

- Due to the varying heights, the pylons do not have equal stiffness and will not deform identically.
- The pylons are not linked rigidly due to the incorporation of the sliding mechanism.
- The special stiff seventh pylon forms part of the structure but, because of the sliding mechanism, it takes some time to start playing its role.
- The oscillation periods are long, and implementation of the behaviour factor will not have a significant influence.

DISCUSSION OF ANALYSIS RESULTS

Loading cases for operational conditions

Wind actions

For the wind loading analyses during the operational stage, along-wind forces similar

Table 11 Forces in the pylons, with full and reduced E modulus, for seismic action

| Model | Model A (beams) Full E | | Model A (beams) Reduced E | | Model A (beams) E | | Full E | Reduced E | Moment ratio |
|--------|------------------------|-------|---------------------------|-------|-------------------|-----------|--------|-----------|--------------|
| | T (s) | M (%) | T (s) | M (%) | Pylon/Cases/Info | | | | |
| Mode 1 | 3.0 | 36.0 | 4.9 | 42.8 | Pylon 1 | Seismic X | 12 322 | 8 301 | 67 |
| Mode 2 | 1.7 | 44.6 | 2.3 | 47.1 | Pylon 2 | Seismic X | 11 144 | 8 159 | 73 |
| Mode 3 | 1.3 | 47.0 | 1.6 | 50.7 | Pylon 3 | Seismic X | 9 520 | 8 082 | 85 |
| Mode 4 | 1.1 | 48.3 | 1.5 | 51.4 | Pylon 4 | Seismic X | 7 465 | 8 446 | 113 |
| Mode 5 | 1.0 | 52.7 | 1.3 | 51.4 | Pylon 5 | Seismic X | 6 235 | 8 608 | 138 |
| Mode 6 | 1.0 | 56.9 | 1.0 | 51.6 | Pylon 6 | Seismic X | 5 902 | 3 913 | 66 |
| Mode 7 | 0.9 | 56.9 | 1.0 | 55.9 | Pylon 7 | Seismic X | 9 580 | 9 485 | 99 |

T – Period of oscillation; M – mass participation; Mx – moment about X axis; My – moment about Y axis

to those in the construction stage are applied to the pylons. Two FE models were analysed:

- Model A1, the FE model with single beam elements and automatic gap elements
- Model B1, the FE model with 3D trusses and beams, and with automatic gap elements.

A summary of the results for the wind actions in the X-direction is shown in Table 12.

Seismic actions

The parameters used for the seismic analyses during the operational life of the structure are identical to those used for the analyses during the construction stage. The acceleration $a = 0.05$ g and the behaviour factor is equal to one. Two FE models were considered and analysed. Model A2, the model with beam elements and soft beams, was analysed first. From the modal analyses, the natural frequencies of each pylon were determined. Using this information, the equivalent static lateral forces for each pylon were calculated and applied in the FE beam model with automatic gap elements, Model A1. A summary of the results for seismic action in the X-direction is given in Table 13. Some of the results differ by up to 10% because, in order to calculate equivalent static lateral forces by hand, it is assumed that the whole mass of each pylon is subjected to the same pseudo-acceleration. This FE model has a more representative mass distribution, leading to more accurate results.

To investigate the effects of seismic action in the Y-direction, analysis was done with all previously mentioned models and the results were almost identical. This is because the flexural stiffness of the gantries is much smaller than that of the pylons, and the gantries do not restrain the pylons. In this case even the model with the automatic gap elements, Model A2, gave very good results, because the pylons on their own act like pure vertical cantilevers during modal analyses. A summary of the results of only one FE model is shown in Table 14.

Comparison of results from the FE models with and without a gap

FE models with soft beams

The modelling of the sliding connection behaviour was a major focus of this work. To highlight the diversity of results between the FE models with and without gaps, Tables 15 and 16 are presented. Table 15 compares the spectral analysis results for the FE models with and without soft beams. Even though the period of oscillation in the FEM without a gap is shorter and therefore the applied lateral load is larger, the bending moment in the first pylon is much smaller. In this case

Table 12 Forces in the pylons from wind analyses during operational conditions

| Model | | Model A1 (beams) | | | Model B1 (3D truss + beams) | | |
|------------------|--------|------------------|---------|----------|-----------------------------|---------|----------|
| Direction | | X | | | X | | |
| Pylon/Cases/Info | | Fz (kN) | Fx (kN) | My (kNm) | Fz (kN) | Fx (kN) | My (kNm) |
| Pylon 1 | Wind X | 30 | 599 | 15 903 | 30 | 596 | 15 653 |
| Pylon 2 | Wind X | 57 | 568 | 14 770 | 60 | 564 | 14 483 |
| Pylon 3 | Wind X | 23 | 538 | 13 854 | 25 | 534 | 13 570 |
| Pylon 7 | Wind X | 44 | 374 | 5 679 | 52 | 405 | 6 325 |

F(x or z) – force in X or Z direction; My – moment about Y axis

Table 13 Forces in the pylons from seismic action in the X-direction

| Model | | Model A2 (beams + soft beams) | | | Model A1 (beams + gap) | | |
|------------------|-----------|-------------------------------|---------|----------|------------------------|---------|----------|
| Direction | | X | | | X | | |
| Pylon/Cases/Info | | Fz (kN) | Fx (kN) | My (kNm) | Fz (kN) | Fx (kN) | My (kNm) |
| Pylon 1 | Seismic X | 26 | 350 | 12 322 | 11 | 329 | 11 522 |
| Pylon 2 | Seismic X | 31 | 322 | 11 144 | 21 | 322 | 10 825 |
| Pylon 3 | Seismic X | 25 | 308 | 9 520 | 6 | 324 | 10 454 |
| Pylon 7 | Seismic X | 9 | 592 | 9 580 | 13 | 653 | 8 944 |

F(x or z) – force in X or Z direction; My – moment about Y axis

Table 14 Forces in the pylons from seismic action in the Y-direction

| Model | | Model A1 (beams + soft beams) | | | |
|------------------|-----------|-------------------------------|----------|----------|----------|
| Direction | | Y | | | |
| Pylon/Cases/Info | | Fy (kN) | Mz (kNm) | My (kNm) | Mx (kNm) |
| Pylon 1 | Seismic Y | 444.49 | 1 615.6 | -0.01 | 15 088 |
| Pylon 2 | Seismic Y | 511.71 | 754.2 | -0.01 | 20 619 |
| Pylon 3 | Seismic Y | 488.7 | 1 125.2 | -0.02 | 18 574 |
| Pylon 7 | Seismic Y | 660.9 | 1 195.1 | -0.24 | 11 335 |

Fy – force in Y direction; M(x,y or z) – moment about X, Y or Z axis

the gantries are effectively tying the pylons and transferring the force to the stiffest seventh pylon.

FE models with automatic gap elements

To perform a more direct comparison, the results of the modal analysis from the FEM with soft beams are used and the same equivalent lateral static load is applied to the FE model with automatic gap elements and the one without gap elements. The results are presented in Table 16. It can be seen that the moment in the first pylon is 2.5 times smaller, while the moment in the seventh pylon is 2.25 times larger. The difference between the force distributions is a result of the presence of the sliding joint. The shear force from seismic loading in the system without sliding connections will travel to the

stiff pylon. On the other hand, in the system with sliding connections, the shear force induced by seismic action will be distributed to each pylon before the sliding mechanism is locked. The force distribution depends on the stiffness of each pylon.

Load combinations

For concrete structures it is common practice to perform only linear static analyses, and then linearly combine the resulting forces and moments of individual load cases in load combinations. In the case of models of structures with gap elements, this approach does not apply, because the behaviour of sliding connections is non-linear. The effect of each load case is analysed in sequence and each load combination must be analysed individually.

Table 15 Comparison between models with and without gap elements (different modal analyses)

| Model | | Model A2 (beams + soft beams) | | | Model A (beams, no gap) | | | Moment ratio |
|-------------------|-----------|----------------------------------|------------|-------------|----------------------------|------------|-------------|-----------------|
| Direction | | X | | | X | | | |
| Column/Cases/Info | | Fz (kN) | Fx (kN) | My (kNm) | Fz (kN) | Fx (kN) | My (kNm) | (%) |
| Pylon 1 | Seismic X | 26 | 350 | 12 322 | 60 | 321 | 6 340 | 51 |
| Pylon 7 | Seismic X | 9 | 592 | 9 580 | 178 | 860 | 15 870 | 166 |

F(x or z) – force in X or Z direction; My – moment about Y axis

Table 16 Comparison between models with and without gap elements (same lateral load is applied)

| Model | | Model A1 (beams + gap) | | | Model A (beams, no gap) | | | Bending ratio |
|-------------------|-----------|------------------------|------------|-------------|-------------------------|------------|-------------|------------------|
| Direction | | X | | | X | | | |
| Column/Cases/Info | | Fz (kN) | Fx (kN) | My (kNm) | Fz (kN) | Fx (kN) | My (kNm) | (%) |
| Pylon 1 | Seismic X | 11 | 329 | 11 522 | 27 | 219 | 4 620 | 40 |
| Pylon 7 | Seismic X | 13 | 653 | 8 944 | 159 | 1 238 | 20 110 | 225 |

F(x or z) – force in X or Z direction; My – moment about Y axis

CONCLUSION

The extensive structural analysis with FEM support used as input in the design for the Medupi Power Station inclined coal conveyor support structures has been outlined in this paper.

Important conclusions on the use of FEMs with varying complexity, considerations for the construction stage loading, the modelling of the sliding connection in the structure and the modelling of the stiffness reduction due to cracked concrete sections were reached.

Finite element modelling of the inclined coal conveyor structure

Regarding the FE modelling and comparison between different FEMs, it is shown that the simplified beam element models provide adequate modelling of the structural behaviour for this kind of structure. Simplified models using beam elements instead of 3D models with shell elements for box sections must be approached with caution, however, because of localised stress concentrations. For the modelling of the steel gantries, the effects of 3D space trusses have to be considered. The simplest model with only one pylon and spring support representing the rest of the structure can be used for preliminary design. The differences in the results obtained are relatively small.

For the final analysis of the overall behaviour of the structure, it is recommended to use the FE model in which the pylons are modelled with beam elements and the gantries are modelled as 3D trusses, i.e. Model C. For the final design of the concrete pylon

box sections, additional FE models with shell elements should be used to perform micro-modelling in order to obtain realistic shear lag effects and localised stress concentrations due to the stiff corner parts of the box sections.

Construction stage loading

The loading and behaviour for both the construction stage and the operational stage were considered. The concrete pylons, being tall and slender structures, should be checked for possible vortex-shedding effects and it was shown that the additional forces induced by these effects could not be neglected. The wind loading is the most critical loading factor during the construction stage. If the ground acceleration is higher than 0.5 g, then seismic loading could become the most critical loading condition.

Modelling of the gantry sliding connection

The impact of detailed aspects of the structural system, such as the sliding and locking mechanism linking the gantries to the concrete pylons, implied that special modelling techniques were required. The non-linear mechanical aspects of the behaviour of the structure for both static and dynamic loading conditions also needed to be dealt with. Using an iterative process, the sliding mechanism modelled with the gap elements can be approximated by 'soft' beams, which are linear elements. With implementation of soft beams the analyst was then able to perform the modal and

response spectrum analyses using standard FE software.

It was shown that the overall behaviour of the structure can be highly influenced by the action of the sliding mechanism and that the force distribution between the structural members can differ significantly.

It is recommended that, if possible, the automatic gap elements that are part of FEM software should be used for static loading. Because these automatic gap elements are non-linear, each load combination must be analysed separately. For dynamic analyses, such as modal and response spectrum analyses, it is recommended that soft beams be used to calculate the periods of oscillation and force distribution. Additional hand calculations using the equivalent lateral force method can be performed to compare the results from the response spectrum analysis with the FEM results.

Effects of stiffness reduction due to cracking of the pylon box section

The effects of reduced stiffness of concrete sections due to cracking were analysed. The reduction in stiffness makes the oscillation periods longer and as a result the computed lateral seismic loading is smaller. The reduction in bending moments in the tallest column was about 30%.

ACKNOWLEDGEMENTS

The permission granted by Eskom Central Power Generation Office to publish this paper is gratefully acknowledged.

The authors of the paper would like to specially thank Prof Johan Retief from the University of Stellenbosch and Mr Hein Barnard, Principle Specialist from AECOM SA, for their support and valuable contribution.

LIST OF SYMBOLS

| | |
|----------|------------------------------------|
| $w_m(z)$ | Mean hourly wind load |
| ρ_a | Air density |
| $v(z)$ | Wind speed at height z |
| C_D | Shape factor |
| $d(z)$ | Width of the section |
| $w_g(z)$ | Wind load due to gust |
| G | Gust factor |
| h | Height of the top of the structure |
| F_x | Force in global X direction |
| F_y | Force in global Y direction |
| F_z | Force in global Z direction |
| ICC | Inclined coal conveyor |
| S(X) | Seismic load in global X direction |
| S(Y) | Seismic load in global Y direction |
| ULS | Ultimate limit state |
| FEM | Finite element model |

FEA Finite element analysis
 $V_{crit,i}$ Critical wind velocity for vortex-shedding
 V_b Basic wind velocity
 a Allowable sliding length
 b Reference width of the cross section
 n Natural frequency
 St Strouhal number
 E Young's modulus of elasticity
 I Moment of inertia
 L Length
 z Height above ground level
 m Mass of a beam
 M_x Moment about global X axis

M_y Moment about global Y axis
 M_z Moment about global Z axis
SLS Serviceability limit state
DLL Dead load
VL Vertical load

REFERENCES

- Autodesk 2015. Autodesk Robot Structural Analysis Professional. Available at: <http://www.autodesk.com/products/robot-structural-analysis>.
- CICIND (International Committee on Industrial Chimneys) 2001. *Model Code for Concrete Chimneys. Part A*. Ratingen, Germany: CICIND.
- EN 1991. *EN-1991-1-4. Eurocode 1: Actions on Structures. Part 1-4: General Actions – Wind Conditions*. Brussels: European Committee for Standardization (CEN).
- SANS 1989. *SANS 0160-1989. The General Procedure and Loading to be adopted in the Design of Buildings*. Pretoria: South African Bureau of Standards.
- Strand7 2015. Finite Element Analysis Software. Available at: <http://www.strand7.com>.
- TNO Diana 2015. Finite Element Analysis Software. Delft, Netherlands. Available at: <http://www.tnodiana.com>.